

# **Rapid/Dynamic Wetting of Molten Slag Droplets on Refractory Surfaces**

C. Nexhip and S. Sun

G. K. Williams CRC for Extractive Metallurgy  
CSIRO Division of Minerals, Box 312  
Clayton South, Vic. 3169, Australia  
Fax : (+613) 9562 8919

## **ABSTRACT**

The physico-chemical properties of liquid slags, and refractory brick composition, play a critical role in influencing the driving forces for wetting and spreading of slags, and hence their likelihood and extent of penetration into refractory bricks. The authors present a technique for measuring the rapid/dynamic contact angle (wetting) of molten  $\text{Na}_2\text{O-B}_2\text{O}_3$  and  $\text{CaO-SiO}_2\text{-Al}_2\text{O}_3\text{-MgO}$  slag droplets contacting solid substrates, as a function of time, temperature, slag chemistry and substrate type. During the initial time period immediately following contact, wetting of the substrate by the liquid slag was generally very rapid, reaching an equilibrium state within  $t < 0.5$  second, even for relatively viscous systems. Calculated dynamic wetting rates ( $d\theta/dt$ ) for a “model”  $\text{Na}_2\text{O-B}_2\text{O}_3$  melts varied from  $\sim 130 - 200$   $^\circ/\text{sec}$  at  $850$   $^\circ\text{C}$  and  $\sim 430 - 600$   $^\circ/\text{sec}$  at  $1000$   $^\circ\text{C}$ , when the  $\text{Na}_2\text{O}$  content was increased from  $9.9 - 16.2$  wt %. The calculated  $d\theta/dt$  thus increased with increasing slag temperature and  $\text{Na}_2\text{O}$  concentration. Dynamic wetting experiments were also performed on porous refractory surfaces, rather than fused/solid oxide substrates associated with conventional equilibrium sessile drop techniques. Calculated  $d\theta/dt$  values for 28wt%  $\text{CaO-42SiO}_2\text{-20Al}_2\text{O}_3\text{-10MgO}$  slag droplets on an inert platinum substrate, were found to be lower than those measured contacting a porous magnesia refractory, irrespective of slag temperature between  $1300 - 1450$   $^\circ\text{C}$ . The work has shown that non-equilibrium slag wetting dynamics can be studied, and quantified using the developed technique.

# 1. INTRODUCTION

Physico-chemical processes such as the penetration of slag melts into the pores and cracks of refractory bricks play an important role in the wear of slag belt linings in furnaces. In metallurgical processes equilibrium is often not attained, thus the kinetics of wetting of slags on refractories is of considerable significance. For instance, the extent of penetration of slag into a particular refractory type will depend on many factors, such as brick porosity, slag composition and temperature. However, the initial contact behaviour between slag and a refractory, (thus the affinity of the slag to wet the brick), will ultimately determine the extent of slag penetration into the refractory pores. Only after this initial contact event can slag then infiltrate the brick, for instance under capillary forces, leading to their subsequent dissolution and degradation, either due to chemical attack or physical erosion.

It is for this reason that interfacial phenomena such as dynamic/non-equilibrium wetting of slags on refractory surfaces should be deemed important, as such phenomena occur during the “original wetting” period,<sup>1)</sup> which is generally prior to chemical reaction induced changes in system wettability. Rather than focus on sessile drop-type experiments to measure the equilibrium contact behaviour of slags on refractories,<sup>2,3)</sup> this paper describes preliminary results of dynamic/non-equilibrium wetting studies on a “model”  $\text{Na}_2\text{O-B}_2\text{O}_3$  system, as a silicate analogue, up to 1000 °C on inert platinum substrates, and also a “secondary steel-making” type slag on platinum and industrial/porous refractories up to 1450 °C. By measuring and analysing the rapid change in contact angle-time behaviour of slags initially contacting fresh refractory surfaces, as a function of slag composition and temperature, it is eventually hoped to quantify and predict the penetration behaviour of industrial slags into porous refractory bricks.

## 2. EXPERIMENTAL

### 2.1 Dynamic Wetting Apparatus and Procedure

The rapid wetting studies involved using two experimental techniques, namely a high temperature furnace with slag droplet device and refractory sample; and a video imaging and analysis system. Experiments were performed in air inside a muffle furnace housing  $\text{MoSi}_2$  heating elements, the furnace having two horizontal optical glass “sighting” tubes to allow visual observations of the wetting experiments within the furnace hot-zone. Figure 1 shows a schematic of the apparatus, where a firebrick structure is used to support a crucible/slag reservoir, located directly above a platinum or refractory tile.

The experiments on  $\text{Na}_2\text{O-B}_2\text{O}_3$  melts were performed in air, and consisted of melting about 1 – 1.5 g of slag powder in a platinum crucible (15 mm height and 19 mm ID). The crucible had a 3 mm hole drilled in the middle of the base, for the droplets to detach. For the  $\text{CaO-SiO}_2\text{-Al}_2\text{O}_3\text{-MgO}$  slag experiments, an alumina crucible (20 mm high and 16.5 mm ID) was used to contain the slag, having a 1 mm hole drilled in the base. For all experiments, an alumina rod (3 mm ID, 5 mm OD), its tip sealed and coated with platinum foil, was used to “plug” the small hole in the base of the crucibles, hence preventing the premature release of liquid from the reservoir. When the desired experimental temperature was attained, the alumina rod, which protruded through the top of the furnace, could be vertically positioned to “unplug” the hole in the crucible, thus releasing a droplet of liquid slag onto the substrate below. The inert

platinum substrate/tile, or samples of refractory brick were situated about 10 mm directly below the hole in the base of the crucible. An R-type thermocouple was also situated immediately below the substrate samples for measuring the temperature. The furnace control thermocouple (R-type), situated inside the furnace hot-zone adjacent to the crucible, was used to estimate the temperature of the slag.

The imaging system comprised a monochromatic CCD video camera (Pulnix, Model no. TM6-CN), having a diode array size of 768 x 512 pixels. Attached to the rear of the camera was a manual shutter controller, allowing the user to select between the standard 1/60, up to a fixed shutter of 1/10,000 seconds. A 75 mm zoom lens, two focal-length extenders (x 2) and a 49 mm close-up lens were also used to image the droplets. The camera system was linked to a date-time generator to provide a readout of the elapsed experimental time, the experiments being recorded using a standard VHS video recorder. The muffle furnace, camera and lenses were all mounted on a vibration-free (N<sub>2</sub>-gas stabilised) optical bench-top, measuring 2.0 m x 1.5 m.

Following a successful high temperature experiment, a PC-driven 8-bit frame grabber (Vision Ezy, DT-55) with image analysis software (Global Lab image v 3.0) was used to capture/digitise each video image of the slag droplet contacting the sample substrate, at 1/25 second intervals (40 milliseconds). This process would continue until  $t \sim 8$  seconds after initial contact was made, when the droplet contact angle appeared to have reached equilibrium. Once the individual video images were saved in digital (\*.tif) format, the image analysis software was used to measure the contact angle ( $\theta$ ) of the slag droplet contacting the horizontal substrate (see Figure 1). The radius of the base of the droplet ( $r$ ) could also be measured, as the thickness of the substrate acted as a distance/thickness calibration. However, these results are not presented in this paper. Due to the viscous nature of the slag systems used (up to  $\sim 4$  Pa.s), it was found that the initial contact velocity between the advancing slag drop and sample base was quite slow, i.e., of the order of mm/sec, hence there was no evidence of droplet deformation usually associated with a high impact velocity. The use of viscous systems such as Na<sub>2</sub>O-B<sub>2</sub>O<sub>3</sub> melts or a CaO-SiO<sub>2</sub>-Al<sub>2</sub>O<sub>3</sub>-MgO slag, also proved convenient due to the limited speed of the conventional video camera used for these experiments (eg. 25 frames/sec).

Wetting experiments were initially performed using a Na<sub>2</sub>O-B<sub>2</sub>O<sub>3</sub> “model” system, as the physico-chemical properties are well-documented in the literature in terms of melt surface tension,<sup>4)</sup> density<sup>5)</sup> and viscosity.<sup>6)</sup> The melt compositions used were 9.9, 13.8 and 16.2 wt % Na<sub>2</sub>O, and experiments were performed at 850 – 1000 °C on a smooth platinum substrate, whose rectangular dimensions were 25 mm x 19 mm x 0.4 mm. The use of a platinum substrate served two purposes : (1) a conveniently smooth/uniform substrate for trialing the technique and, (2) the platinum is chemically inert, hence eliminating the likelihood of any chemical reaction occurring between the liquid and solid. Thus the effect of the physico-chemical properties of the liquid slags on the driving force for “original wetting”<sup>2)</sup> could be studied unambiguously.

Preliminary experiments were also performed in air using a 28wt%CaO-42SiO<sub>2</sub>-20Al<sub>2</sub>O<sub>3</sub>-10MgO secondary steel-making slag system at 1300 – 1450 °C. Wetting dynamics were studied using the platinum substrate, and also industrial (< 18 % porosity) refractory substrates (RADEX-AS90-S), the brick composition being 92 % MgO and 6.5 % Al<sub>2</sub>O<sub>3</sub>, with  $\sim 0.5$  % Fe<sub>2</sub>O<sub>3</sub>, 0.9 % CaO and 0.2 % SiO<sub>2</sub>. The refractory tiles were cut using a diamond saw, to dimensions of 24 mm x 19 mm x 4.5 mm. A crude estimate of the slag droplet mass

was also made using knowledge of the liquid density at a particular temperature and the initial radius of the droplets from the captured images. For either the borate or silicate systems, the droplet mass was generally between  $\sim 200 - 800$  mg, and was found to be difficult to reproduce.

## 2.2 Preparation of $\text{Na}_2\text{O-B}_2\text{O}_3$ and $\text{CaO-SiO}_2\text{-Al}_2\text{O}_3\text{-MgO}$ Slags

Samples were prepared using sodium tetra-borate,  $\text{Na}_2\text{B}_4\text{O}_7 \cdot 10\text{H}_2\text{O}$  (Univar, 99.5 % purity) as the starting material. Impurity levels quoted by the manufacturer were  $\text{PO}_4^{3-}$  (0.001 %) and  $\text{SO}_4^{3-}$  (0.005 %). Additions of boric acid,  $\text{H}_3\text{BO}_3$  (BDH, 99.8 % purity) were made to achieve the intended  $\text{Na}_2\text{O-B}_2\text{O}_3$  melt compositions of 9, 14 and 18 wt %  $\text{Na}_2\text{O}$ . The main impurities within the boric acid (quoted by the manufacturer) were  $\text{PO}_4^{3-}$  (0.005 %) and  $\text{SO}_4^{3-}$  (0.005 %). Compositions were chosen within the range where literature data on surface tension, density and viscosity of the system were readily available. Samples were well mixed and pre-melted in a Pt/30%Rh crucible in a “pot” furnace at 1323 K in air. The solidified glassy samples were pulverised using a WC ring-mill and then sieved through a 200  $\mu\text{m}$  mesh, and finally remelted in air to ensure homogeneity. The samples were ready to use after quenching on a copper plate in air, followed by pulverisation. Using Atomic Absorption Spectrophotometry and Inductively Coupled Plasma, analyses of the samples showed the final borate compositions as 9.9 wt %, 13.8 wt % and 16.2 wt %  $\text{Na}_2\text{O}$ .

The  $\text{CaO-SiO}_2\text{-Al}_2\text{O}_3\text{-MgO}$  slag was prepared by using AR-grade  $\text{SiO}_2$ ,  $\text{Al}_2\text{O}_3$  (BDH, 99.3 % purity) and dried AR grade  $\text{CaCO}_3$  and  $\text{MgCO}_3$  powders as the starting materials. Powders were initially weighed, mixed thoroughly and then melted in a platinum crucible in air using a muffle furnace at 1500  $^\circ\text{C}$ . The samples were ready to use after quenching on a cold copper plate in air, followed by pulverisation. The slag had an intended composition of 28wt%CaO–42  $\text{SiO}_2$ –20 $\text{Al}_2\text{O}_3$ –10MgO.

## 3. RESULTS and DISCUSSION

### 3.1 Dynamic Wetting of $\text{Na}_2\text{O-B}_2\text{O}_3$ Melts on a Platinum Substrate

Some video images captured during a dynamic wetting experiment using a  $\text{B}_2\text{O}_3$ -16.2 wt %  $\text{Na}_2\text{O}$  melt at 950  $^\circ\text{C}$ , (for instance), are shown in Figure 2. A series of wetting profiles ( $\theta$  versus  $t$ ) at different temperatures can be seen in Figure 3, where the contact angle was obtained by repeated (10) measurements on each captured image. The contact angle of the droplets appear to reach a constant/equilibrium value within an elapsed time of  $t \sim 0.5$  seconds. Figure 3 also shows the apparent equilibrium contact angle ( $\theta_e$ ) to decrease with increasing temperature, ie.,  $\theta_e \sim 48^\circ$  and  $\theta_e \sim 12^\circ$  at 850  $^\circ\text{C}$  and 1000  $^\circ\text{C}$ , respectively.

To determine the dynamic wetting rate ( $d\theta/dt$ ), the slope of the contact angle versus time data during the initial stage was calculated. Figure 4 shows the initial contact angle versus time data for the  $\text{B}_2\text{O}_3$ -16.2 wt %  $\text{Na}_2\text{O}$  melt at 850  $^\circ\text{C}$ , where the wetting rate is calculated to be  $d\theta/dt \sim 195^\circ/\text{sec}$ . The initial region was defined as the time period from immediate contact where  $\theta$  versus time data was most linear, until an observed inflection/transition region where the  $\theta$  versus time data is observed to deviate from linearity (thus  $\theta \rightarrow \theta_e$ ) until an equilibrium angle is attained. The results for the dependence of dynamic wetting rate, as a function of

Na<sub>2</sub>O-B<sub>2</sub>O<sub>3</sub> melt composition and temperature can be seen in Table I and Figure 5. It should be noted that the  $\pm$  error expressed for each  $d\theta/dt$  in Table I was calculated for a 95 % confidence interval. It can be observed from Figure 5, that the logarithm of the dynamic wetting rate ( $d\theta/dt$ ) increases linearly with increasing reciprocal temperature of the melt ( $1/T$ ). For instance, when the temperature is increased from 850 – 1000 °C, the rate increases by about 300 %, while for a given temperature of 850 °C,  $d\theta/dt$  increases by 45 %, when the concentration of Na<sub>2</sub>O is increased from 9.9 – 16.2 wt %.

According to the work of Shartsis and Capps,<sup>6)</sup> within the temperature range of this study, the bulk viscosity ( $\mu$ ) of the melts ranges from  $\mu \sim 2.1$  Pa.s down to about 0.25 Pa.s, respectively. The strong dependence of  $d\theta/dt$  on temperature is most likely the result of melt viscosity. However, no direct proportionality is apparent. Using Shartsis and Capps' data, the energy of activation for viscous flow ( $E_{a\mu}$ ) can be estimated to be around 200 kJ/mol for the B<sub>2</sub>O<sub>3</sub>-16.2 wt % Na<sub>2</sub>O melts (for example). The Arrhenius plots in Figure 5 reveal the energies of activation for dynamic wetting to be  $\sim 80 - 90$  kJ/mol, ie., well below that estimated for viscous flow, thus showing a weaker dependence than proportionality.

The surface tension of the borate melts are also known to decrease<sup>4)</sup> from  $\gamma \sim 150 - 110$  mN/m, with a decrease in Na<sub>2</sub>O concentration from about 20 - 10 wt % Na<sub>2</sub>O at 1000 °C. Figure 6 shows the calculated dynamic wetting rates from Table I, replotted as a function of melt surface tension and temperature. Here it can be seen that the wetting rate decreases reasonably linearly with decreasing melt surface tension (increasing B<sub>2</sub>O<sub>3</sub>) for a given temperature. For instance, at 850 °C, the surface tension of the melts decreases from  $\gamma \sim 140 - 105$  mN/m, when the Na<sub>2</sub>O concentration is decreased from 16.2 – 9.9 wt %, respectively. This results in  $d\theta/dt$  decreasing from around 195 - 135 °/sec. What is also interesting is that if one were to extrapolate the linear regressions of the plots in Figure 6 to the  $x$  – axis, a value of the surface tension when  $d\theta/dt \rightarrow 0$ , can be obtained (defined here as the “critical” surface tension,  $\gamma_c$ ). The slopes of the surface tension versus  $d\theta/dt$  data in Figure 6, also appear to increase with increasing melt temperature. Table II and Figure 7 show the results of the extrapolated  $x$ -intercepts ( $\gamma_c$ ) and the calculated slopes from the  $\gamma$  versus  $d\theta/dt$  plots in Figure 6. Currently, the implications of the results in Table II and Figure 7 are uncertain, and further analysis is required. However, there does appear to be a very linear relationship between the calculated slopes  $[(d\theta/dt)/(mN/m)]$  and the extrapolated critical surface tension values; with the slope  $\rightarrow 0$  at an estimated  $\gamma_c \sim 105$  mN/m.

### 3.2 Dynamic Wetting of a CaO-SiO<sub>2</sub>-Al<sub>2</sub>O<sub>3</sub>-MgO Slag on a Platinum, & Magnesia Porous Refractory

As already mentioned, the advantage of the technique described in this paper, compared with the well-known sessile drop technique, is that the former allows one to study *non-equilibrium* wetting phenomena. As these dynamic wetting experiments occur over a very short time duration (eg. < 1 second, even for viscous systems), it allows rapid contact angle data to be measured, prior to slag infiltration, for droplets contacting porous substrates, as opposed to using fused/high density substrates typically associated with the sessile drop technique. The results for preliminary dynamic wetting measurements on an industrial/porous refractory between 1300 – 1450 °C can be seen in Table III and Figure 8.

Experiments were also carried out using a platinum substrate, and although the wetting profiles ( $\theta$  versus  $t$ ) on platinum are not shown in Figure 8, the calculated wetting rates as a function of temperature are listed in Table III. The results in Figure 8 suggest that the silicate slags show very similar wetting profiles to those observed for the lower temperature borate model system. That is, in the initial non-equilibrium stages of wetting, a reasonably linear relationship is obtained for  $\theta$  versus  $t$ , and can be used to calculate the dynamic wetting rate in the usual manner. Again the  $\pm$  error expressed for each  $d\theta/dt$  in Table III was calculated for a 95 % confidence interval. The equilibrium contact angles (not shown in Figure 8), attained after  $t \sim 4$  seconds, were relatively constant for the platinum substrate ( $\theta_e \sim 49^\circ$ ) between 1300 – 1450 °C. Those measured on the magnesia refractory varied between  $\theta_e \sim 55^\circ$  at 1300 °C, and  $\theta_e \sim 42^\circ$  at 1450 °C. These values are approximations only, as the slag droplets were observed to infiltrate into the porous refractory substrates after a few seconds had elapsed post-contact.

The calculated  $d\theta/dt$  results for the platinum substrate in Table III are lower than those calculated for the porous MgO substrate, the  $\pm$  errors are also lower for the experiments on platinum. When the temperature is increased from 1300 – 1450 °C,  $d\theta/dt$  increases by  $\sim 65\%$  for platinum, but  $\sim 125\%$  for magnesia. The average correlation coefficient derived from the initial wetting rates on the magnesia refractory, observed in Figure 8, was  $r^2 \sim 0.95$ . This is a reasonable result (good linearity), given the droplets are contacting a porous refractory, rather than a dense/fused oxide substrate. This suggests that quantitative  $d\theta/dt$  data can in fact be reliably obtained for industrial porous refractories, rather than using less realistic substrates, provided this initial linear stage of dynamic wetting is used for calculating  $d\theta/dt$ .

Figure 9 and Table III show the effect of temperature and estimated surface tension on the calculated dynamic wetting rate of the 28CaO-42SiO<sub>2</sub>-20Al<sub>2</sub>O<sub>3</sub>-10MgO slag on the platinum substrate and magnesia based refractory. It should be noted that the surface tension values quoted are from unpublished work by the authors using the maximum-pull method. As was observed for the model borate system, Figure 9 also shows  $d\theta/dt$  to increase with increasing slag temperature, and again is most likely the result of bulk viscosity. If one were to plot the logarithm of  $d\theta/dt$  as a function of reciprocal slag temperature (not shown here), then the slope would yield an activation energy for dynamic wetting of  $E_a \sim 90$  kJ/mol. The bulk viscosities for this system have been previously measured<sup>7)</sup> for a very similar slag composition of 30CaO-40SiO<sub>2</sub>-20Al<sub>2</sub>O<sub>3</sub>-10MgO, and ranges from  $\mu \sim 4.4 - 1$  Pa.s, when the temperature is increased from 1300 – 1450 °C, respectively. From this, the energy of activation for viscous flow can be estimated to be  $E_{a\mu} \sim 155$  kJ/mol; the influence of temperature on  $d\theta/dt$  again showing a weaker dependence than proportionality.

The wetting rate in Figure 9 also shows an opposite trend with slag surface tension, when compared to the borate results. That is, for this silicate slag,  $d\theta/dt$  is observed to increase with increasing temperature, but *decreasing* slag surface tension, irrespective of substrate type. As already mentioned, the influence of bulk viscosity on  $d\theta/dt$  appears to be greater than surface tension (showing a weaker dependence than proportionality). Rather than focus on a particular slag composition, as shown here in Figure 9, the dependence of varying slag composition on the wetting rate needs to be investigated, to determine the true effect of other possible driving forces such as slag surface tension.

In the near future, the developed technique will be used to study the rapid/dynamic wetting of iron silicate and calcium ferrite slags on Mag-chrome and MgO based refractories. This will require the control of the furnace atmosphere to vary the iron chemistry, and a very high speed video camera, particularly for the inviscid ferrite systems which can have viscosities similar to liquid metals. Such equipment has now been commissioned within CSIRO Minerals, and experiments have commenced.

In addition, a more accurate technique for producing slag droplets of known volume is being developed. This involves using a pressurized capillary to control the droplet delivery speed (under positive or negative pressure). Hence, unlike the present arrangement using a slag reservoir “plug,” this new device will avoid premature leakage of the slag prior to reaching the desired temperature, or chemical equilibrium in the case of iron-containing slags. The quantitative information gained will then be used to form linkages with other ongoing work in the Centre on slag infiltration, thermal cycling and phase equilibria of industrial refractories.

## 4. CONCLUSIONS

An experimental apparatus has been constructed and used to quantify the dynamic wetting phenomena of slag droplets contacting fresh refractory surfaces as a function of slag composition, temperature and substrate type. Preliminary results have shown :

- During the initial time period immediately following contact, wetting of the substrate by the liquid slag was generally very rapid, reaching an equilibrium state within  $t < 0.5$  second, even for relatively viscous systems.
- Calculated dynamic wetting rates ( $d\theta/dt$ ) for borate melts varied from  $\sim 130 - 200$  °/sec at  $850$  °C and  $\sim 430 - 600$  °/sec at  $1000$  °C, when the  $\text{Na}_2\text{O}$  content was increased from  $9.9 - 16.2$  wt %. The calculated  $d\theta/dt$  thus increased with increasing slag temperature and  $\text{Na}_2\text{O}$  concentration.
- Calculated  $d\theta/dt$  values for  $28\text{wt}\%\text{CaO}-42\text{SiO}_2-20\text{Al}_2\text{O}_3-10\text{MgO}$  slag droplets on a platinum substrate, were lower than those measured on a porous magnesia refractory, irrespective of slag temperature between  $1300 - 1450$  °C.
- The  $d\theta/dt$  values were found to decrease with decreasing surface tension for  $\text{Na}_2\text{O}-\text{B}_2\text{O}_3$  melts, at a constant temperature, while for the  $\text{CaO}-\text{SiO}_2-\text{Al}_2\text{O}_3-\text{MgO}$  slag,  $d\theta/dt$  decreased with *increasing* slag surface tension. This difference is likely to be due to the fact that, unlike the borate melts, the compositional dependence of the silicate slag on  $d\theta/dt$  was not studied, thus only the influence of temperature for a  $28\text{wt}\%\text{CaO}-42\text{SiO}_2-20\text{Al}_2\text{O}_3-10\text{MgO}$  slag. The preliminary results obtained suggest viscosity of the slag has a greater influence on  $d\theta/dt$  than does the surface tension. Further work is required to substantiate the true “driving forces” for dynamic wetting of silicate slags into fresh magnesia-based refractory bricks.

## 5. ACKNOWLEDGEMENTS

Financial support for this work was provided through the Australian Government Cooperative Research Centre Program, through the G. K. Williams CRC for Extractive Metallurgy, a joint venture between CSIRO Minerals and the University of Melbourne (Department of Chemical Engineering). The authors also thank Rowan Davidson and Justen Bremmell for technical support.

## 6. REFERENCES

- 1) H. Fujii and H. Nakae., *ISIJ International*., 1990, vol. 30, p1114.
- 2) J. R. Donald, H. Fukuyama and J. M. Toguri., *EPD Congress, The Minerals, Metals & Materials Society*., 1996, p. 123-135, (Edited by G. Warren).
- 3) H. Fukuyama J. R. Donald, and J. M. Toguri., *EPD Congress, The Minerals, Metals & Materials Society*., 1996, pp. 109-122, (Edited by G. Warren).
- 4) L. Shartsis and W. Capps., *J. Am. Cer. Soc.*, 1952, vol. 35 (7), pp. 169-172.
- 5) L. Shartsis, W. Capps and S. Spinner., *J. Am. Cer. Soc.*, 1953, vol 36 (2), pp. 35-43.
- 6) L. Shartsis, W. Capps and S. Spinner., *J. Am. Cer. Soc.*, 1953, vol. 36 (10), pp. 319-326.
- 7) J. S. Machin and D. L. Hanna., *J. Am. Ceram. Soc.*, 1945, vol. 28, pp. 310-316.



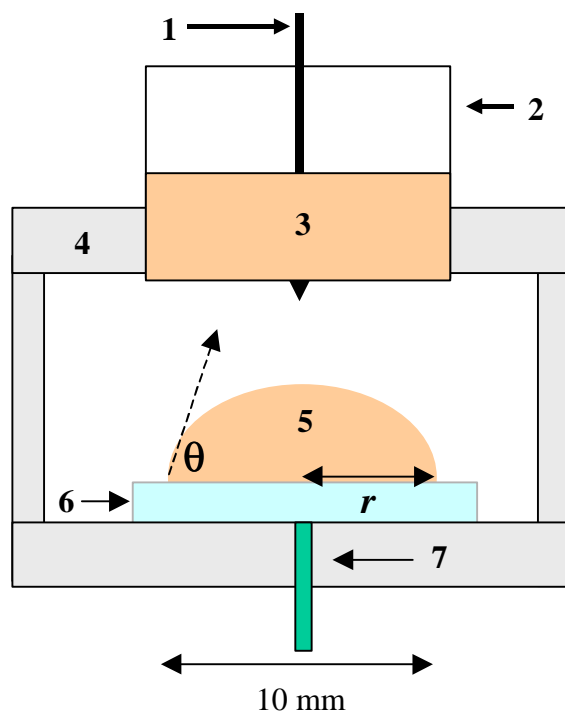


Figure 1. Experimental apparatus used for dynamic wetting studies of slags on solid substrates; (1) reservoir “plug,” (2) platinum or alumina crucible, (3) melt or slag, (4) fire-brick support, (5) droplet, (6) substrate, (7) R-type thermocouple.

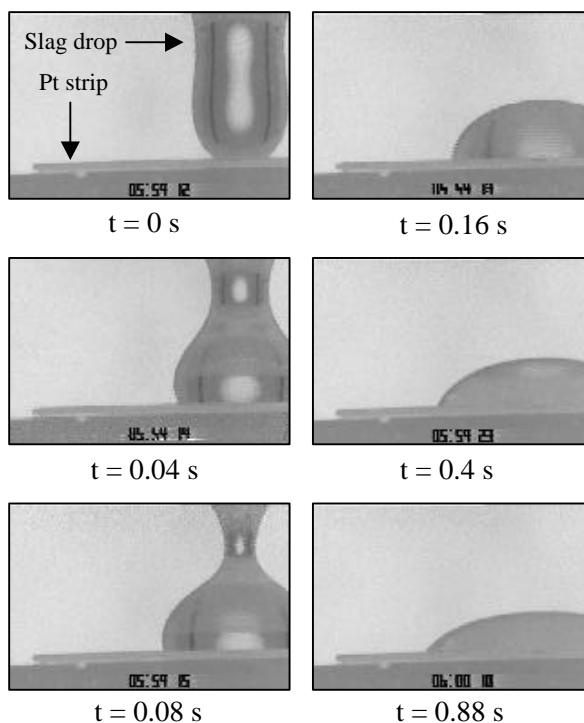


Figure 2. Captured video images of a  $B_2O_3$ -16.2 wt %  $Na_2O$  melt contacting a platinum substrate at 950 °C, as a function of elapsed time (t).

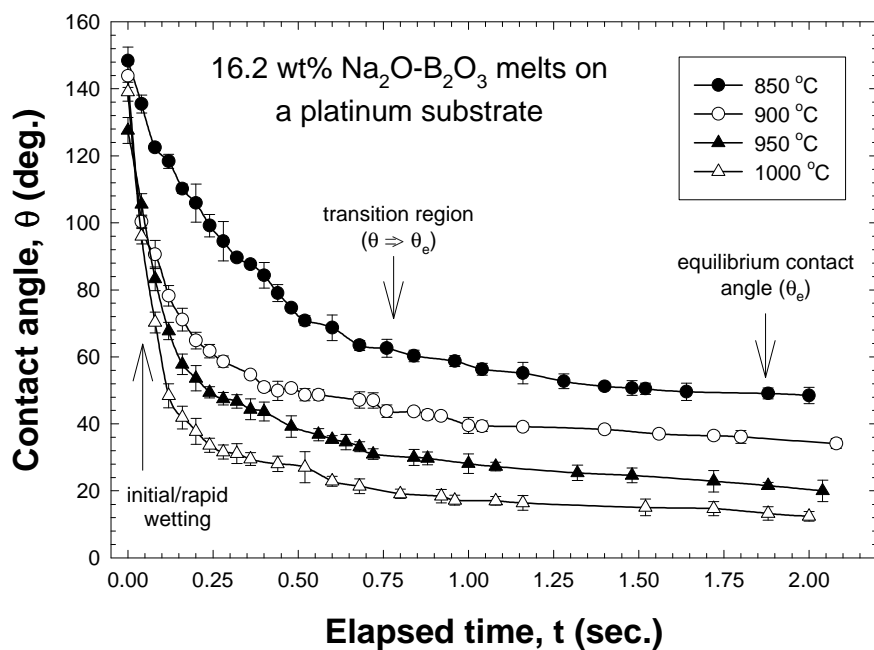


Figure 3. Dynamic wetting profiles ( $\theta$  versus time) for B<sub>2</sub>O<sub>3</sub>-16.2 wt % Na<sub>2</sub>O melts, as a function of temperature on a platinum substrate.

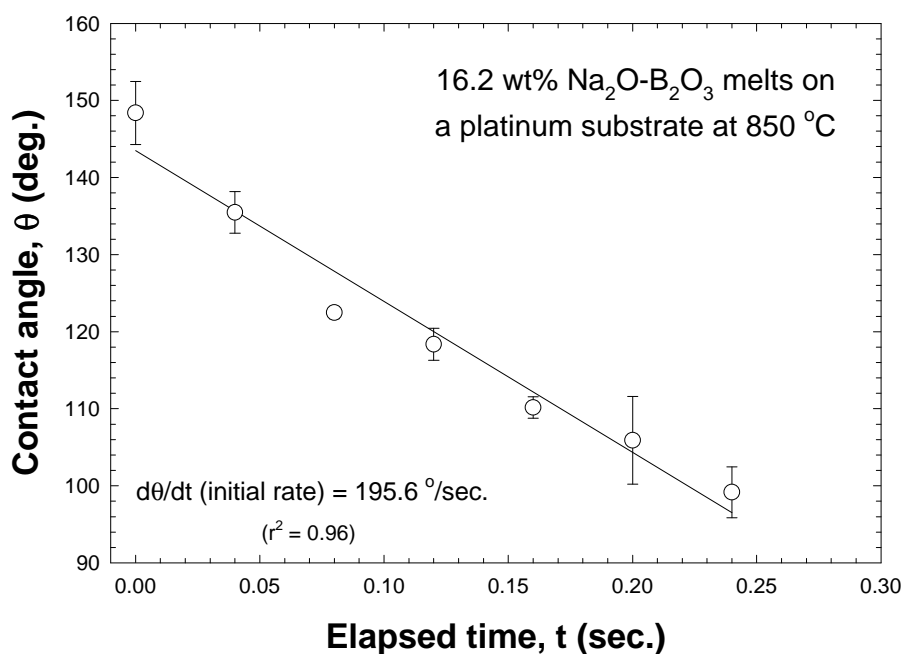


Figure 4. Plot showing how the wetting rate (slope) is calculated during the initial/linear part of the  $\theta$  versus  $t$  profile, for a B<sub>2</sub>O<sub>3</sub>-16.2 wt % Na<sub>2</sub>O melt at 850 °C on a platinum substrate.

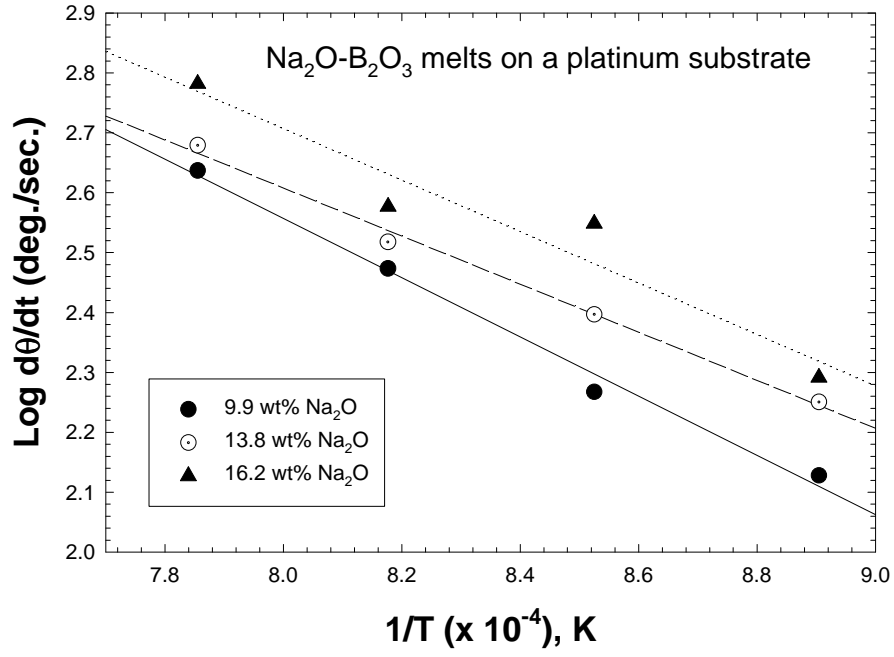


Figure 5. Arrhenius plot of dynamic wetting rate of Na<sub>2</sub>O-B<sub>2</sub>O<sub>3</sub> melts on platinum, as a function of composition and temperature (see Table I).

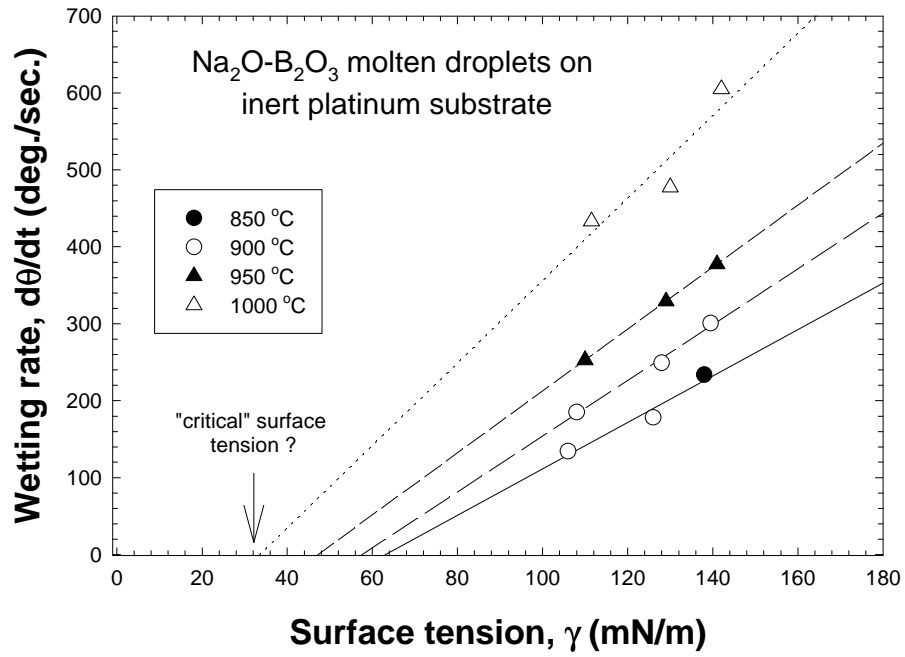


Figure 6. Influence of melt surface tension and temperature on the dynamic wetting rate of Na<sub>2</sub>O-B<sub>2</sub>O<sub>3</sub> melts on a platinum substrate.

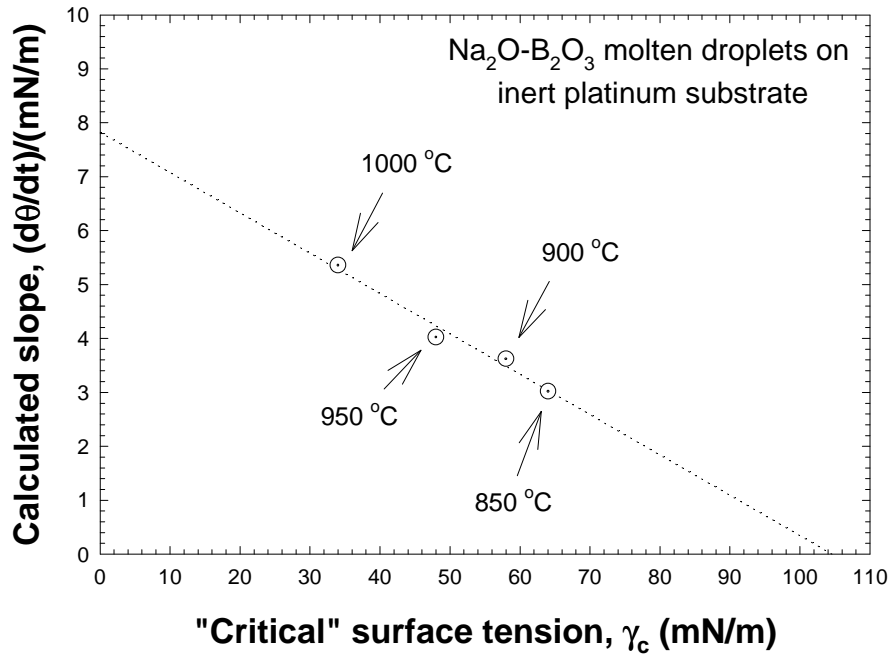


Figure 7. Correlation between extrapolated  $x$ -intercepts ("critical" surface tension,  $\gamma_c$ ) and calculated slopes for  $\gamma$  versus  $d\theta/dt$  data in Figure 6 (see also Table II).

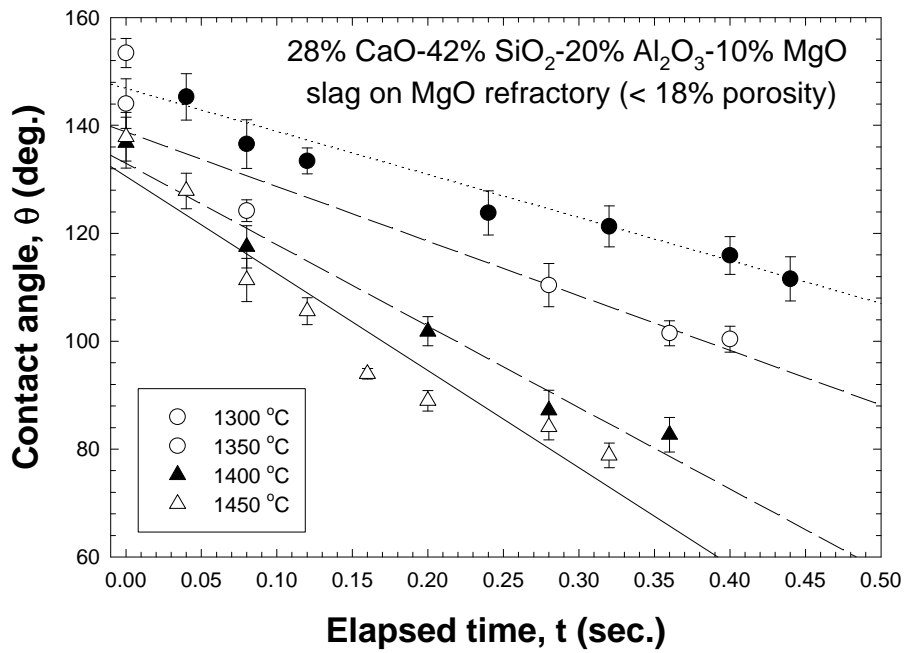


Figure 8.  $\theta$  versus time profiles obtained for a 28wt% CaO-42SiO<sub>2</sub>-20Al<sub>2</sub>O<sub>3</sub>-10MgO slag on magnesia based refractory (< 18 % porosity), as a function of temperature.

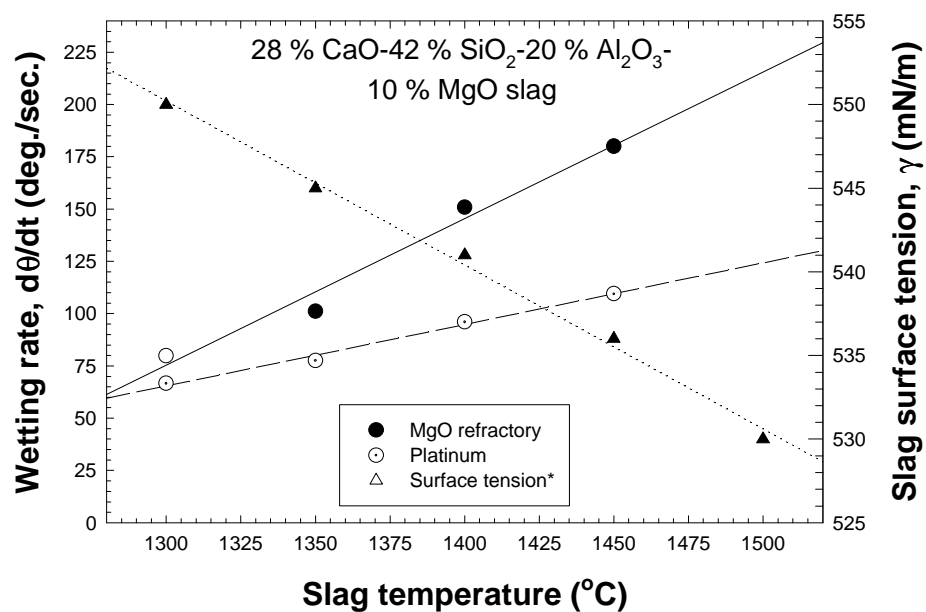


Figure 9. Effect of measured slag surface tension and temperature on the calculated dynamic wetting rate of 28wt%CaO-42SiO<sub>2</sub>-20Al<sub>2</sub>O<sub>3</sub>-10MgO slags on a magnesia based refractory of < 18 % porosity (see also Table III).

Table I. Calculated dynamic wetting rates of Na<sub>2</sub>O-B<sub>2</sub>O<sub>3</sub> melts as a function of composition and temperature, on a platinum substrate.

	<i>B<sub>2</sub>O<sub>3</sub>-9.9 wt % Na<sub>2</sub>O</i>	<i>B<sub>2</sub>O<sub>3</sub>-13.8 wt % Na<sub>2</sub>O</i>	<i>B<sub>2</sub>O<sub>3</sub>-16.2 wt % Na<sub>2</sub>O</i>
<b>Temp. (°C)</b>	<b>Calculated Wetting Rate, dθ/dt</b>	<b>Calculated Wetting Rate, dθ/dt</b>	<b>Calculated Wetting Rate, dθ/dt</b>
850	134.2 ± 32	178.1 ± 43	195.6 ± 45
900	185.0 ± 79	249.3 ± 60	353.5 ± 207
950	297.2 ± 112	329.4 ± 168	377.5 ± 127
1000	433.2 ± 162	477.5 ± 269	605.1 ± 302

(± error in dθ/dt calculated for a 95 % confidence interval)

Table II. Extrapolated *x*-intercepts (“critical” surface tension, γ<sub>c</sub>) versus calculated slope, for γ versus dθ/dt data in Figure 6.

<b>Temp. (°C)</b>	<b><i>x</i>-Intercept, γ<sub>c</sub> (mN/m)</b>	<b>Calc. Slope (dθ/dt).(mN/m)</b>	<b>r<sup>2</sup> value</b>
850	~ 64	3.018	0.955
900	~ 58	3.622	0.991
950	~ 48	4.025	0.999
1000	~ 34	5.359	0.852

Table III. Calculated dynamic wetting rates of a 28wt%CaO-42SiO<sub>2</sub>-20Al<sub>2</sub>O<sub>3</sub>-10MgO slag on platinum and magnesia based refractory (< 18 % porosity), as a function of slag temperature and surface tension.

<b>Temp. (°C)</b>	<b>Calculated Wetting Rate, dθ/dt, on Platinum</b>	<b>Calculated Wetting Rate, dθ/dt, on MgO</b>	<b>Measured Slag Surface Tension,* γ (mN/m)</b>
1300	66.6 ± 8	79.7 ± 17	~ 550
1350	77.6 ± 14	101.2 ± 45	~ 545
1400	93.0 ± 13	150.9 ± 47	~ 541
1450	109.5 ± 46	180.0 ± 53	~ 536
1500	-	-	~ 530

(± error in dθ/dt calculated for a 95 % confidence interval)

(\* = unpublished work by the authors using the maximum-pull method)